PROCEEDINGS OF SCIENCE

Search for Dark Matter and hidden sectors in CMS

Florian Eble[a,*] **on behalf of the CMS collaboration**

[a] *ETH Zürich*

E-mail: florian.eble@cern.ch

Recent results for dark matter (DM) and hidden sectors using the LHC Run 2 data collected by the CMS experiment are presented. Four searches are discussed: DM produced with a pair of W boson, prompt GeV scale di-muon resonance, inelastic DM with displaced muons and resonant production of strongly coupled DM. These searches analyzed proton-proton collision data at a center-of-mass energy of 13 TeV corresponding to an integrated luminosity of 137 fb^{-1} or 96.6 fb^{-1} when using special "scouting" triggers. The dedicated trigger and novel identification and reconstruction algorithms employed in the analyses are discussed. No significant deviation from the Standard Model is observed and exclusion limits for the benchmark new physics models considered are set.

The European Physical Society Conference on High Energy Physics (EPS-HEP2023)
21-25 August 2023
Hamburg, Germany

*Speaker

PoS(EPS-HEP2023)043

1. Introduction

The standard model (SM) of particle physics has been tested experimentally to very high precision and always found in excellent agreement with theoretical calculations. However, it does not explain the existence of dark matter, suggested by astronomical observation such as the cosmic microwave background power spectrum [1]. This motivates to search for dark matter (DM) in the context of physics beyond the SM, in particular in the form of hidden sectors. Hidden sectors consist of DM particles that do not couple to SM fields directly but via a mediator, also called portal. This report presents four searches for hidden sectors, with vector boson portal, using the LHC Run 2 data collected by the CMS experiment [2]. These searches analyzed proton-proton collision data at a center-of-mass energy of 13 TeV corresponding to an integrated luminosity of 137 fb^{-1} or 96.6 fb^{-1} when using special "scouting" triggers.

2. Search for dark matter with particles produced in W^+W^- events

The search presented in this section probes the hypothesis that DM particles χ acquire their mass through interaction with a dark Higgs boson. The signal model used postulates DM particles interacting under a new $U(1)$ local gauge symmetry, which yields a dark Higgs boson singlet s and a massive spin-1 vector boson Z' [3]. The analysis considers dark Higgs masses above 160 GeV, where the branching ratio to W^+W^- is largest. The signatures in which the W bosons both decay to charged leptons and neutrinos (di-leptonic channel), or in which one decays to a charged lepton and a neutrino and the other decays to a pair of jets (semi-leptonic channel) are considered.

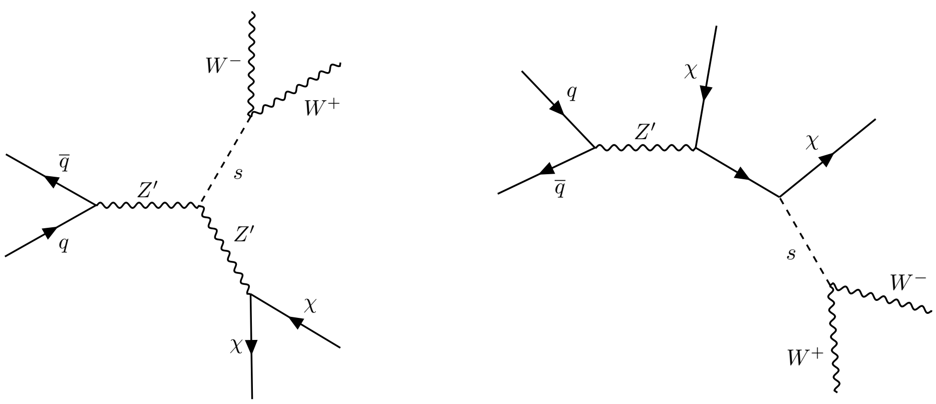

Figure 1: Representative Born-level Feynman diagrams for the benchmark signal model.

In the di-leptonic channel, the observables chosen to test the dark Higgs model are the transverse mass of the trailing lepton plus missing transverse momentum $p_{\mathrm{T}}^{\mathrm{miss}}$ system, $m_{\mathrm{T}}^{\ell_{\mathrm{min}}, p_{\mathrm{T}}^{\mathrm{miss}}}$, and the invariant mass of the di-lepton system $m_{\ell\ell}$. The signal is extracted from a 2D profiled fit, using the asymptotic approximation of the profiled likelihood as a test statistic. In order to account for the dependence of the kinematic properties of the final state objects on the mass of the dark Higgs, the events are further categorized depending on a proxy of the boost of the dark Higgs boson: the

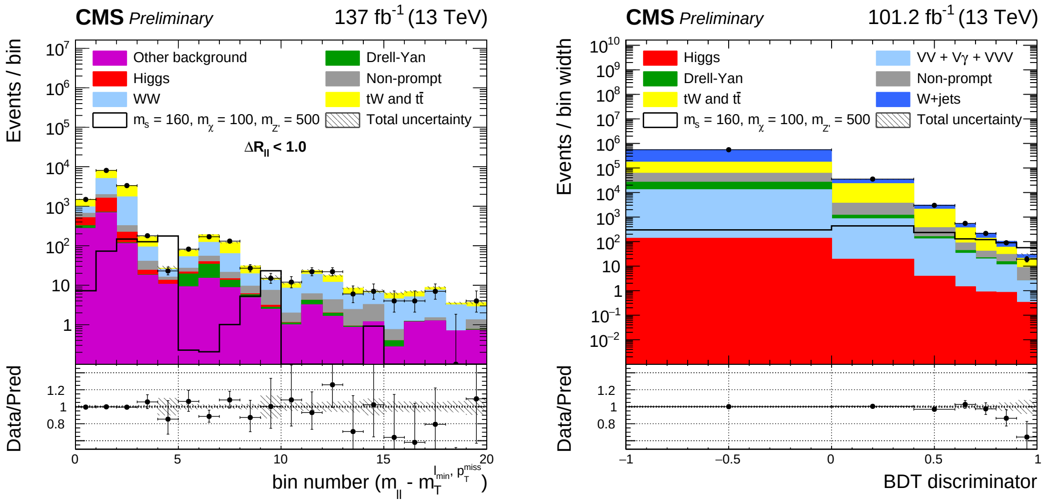

Figure 2: (Left) Unrolled $m_{\ell\ell}$-$m_{\mathrm{T}}^{\ell_{\min},p_{\mathrm{T}}^{\mathrm{miss}}}$ post-fit distributions in the di-leptonic channel for the $\Delta R_{\ell\ell} < 1.0$ signal region. (Right) Post-fit BDT distribution in the semi-leptonic channel for 2017-2018. The signal region has different binning in 2016 and 2017-2018 to ensure good statistical precision in all bins.

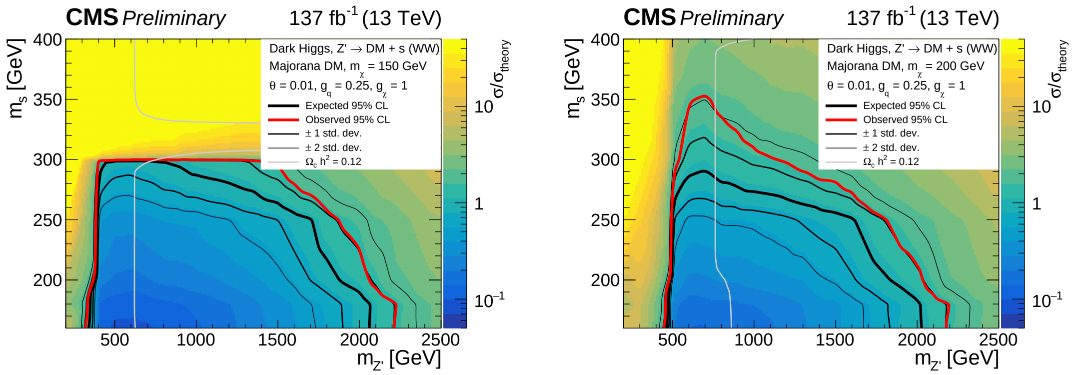

Figure 3: Observed (expected) exclusion regions at 95% CL for the dark Higgs model in the dark Higgs mass and Z' mass plane for DM mass of 150 GeV (left) and 200 GeV (right), marked by the solid red (black) line. The gray line indicates where the model parameters produce exactly the observed relic density $\Omega_c h^2 = 0.12$.

angular distance between the two leptons in the (η, ϕ) plane, $\Delta R_{\ell\ell}$. The expected number of events for signal and background for one bin in $\Delta R_{\ell\ell}$ is provided in Fig. 2.

In the semi-leptonic channel, due to the relatively low cross section of the signal processes and the large irreducible backgrounds, the variables that showed most promising separation of signal and background are combined in a single discriminator using a Boosted Decision Tree (BDT). The expected number of events for signal and background in bins of the BDT score is provided in Fig. 2.

No significant deviation from the SM predictions are observed, and exclusion limits in the dark Higgs mass m_s and Z' mass $m_{Z'}$ plane are shown in Fig. 3. In the case where $m_s \geq 2m_\chi$, the dark Higgs boson decays predominantly to a pair of DM particles, resulting in a sharp drop in sensitivity.

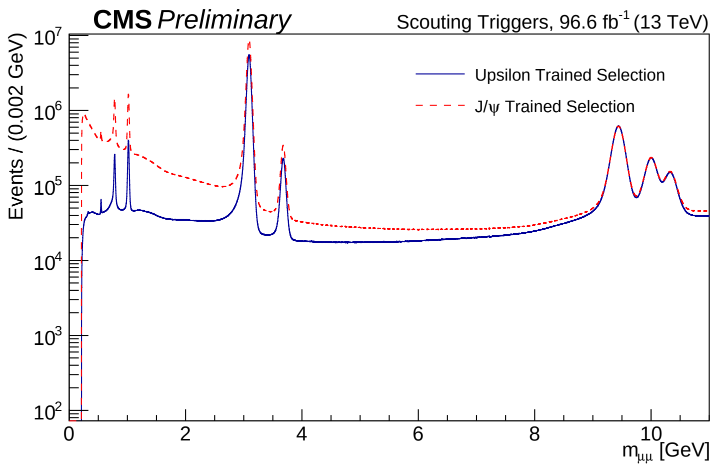

Figure 4: The di-muon invariant mass distribution obtained with the scouting data collected during 2017 and 2018 with two muon identification BDTs.

3. Search for prompt production of a GeV scale di-muon resonance

This analysis is designed to exploit the high integrated luminosity of the LHC to search for a low mass resonance with small effective couplings to the SM sector. A search for a resonance decaying to a pair of muons was performed for masses in the 11.5 to 200 GeV range in Ref. [4]. This analysis targets lower masses, in the 1.1 to 2.6 GeV and 4.2 to 7.9 GeV ranges. These mass windows exclude the J/ψ, ψ' and $\Upsilon(1S)$ resonances. Results are interpreted in the context of a hidden sector with dark photon portal: a new dark field $U(1)_D$ with kinetic mixing with the SM hypercharge gauge field $U(1)_Y$ yields a massive dark photon with suppressed coupling to SM particles. The two main features of this analysis are the usage of so-called "scouting triggers" and of a tailored muon identification algorithm.

Scouting triggers allow to record events with higher rate by trading off for the full event information: all of the event reconstruction is performed by the High Level Trigger (HLT) [5]. This allows to record events with 2 muons with invariant mass above than 1 GeV, while standard triggers limit the di-muon invariant mass to 45 GeV. Because these triggers did not exist in 2016, only 2017 and 2018 data were used for this search, corresponding to an integrated luminosity of 96.6 fb^{-1}.

The muon identification algorithm relies on a tag and probe technique. A BDT is trained on data events with two muons, where one muon passes a cut-based selection (tag). Signal events are events where the second muon has opposite sign and the di-muon invariant mass falls in the J/ψ or $\Upsilon(1S)$ mass window. Background events, enriched with non-prompt and misidentified muons, are formed by events where the second muon has same sign as the probe muon and the di-muon invariant mass is in the 3 to 10 GeV range. Two BDTs are trained in total, one per mass region ($1.1 \leq m_{\mu\mu} \leq 2.6$ GeV and $4.2 \leq m_{\mu\mu} \leq 7.9$ GeV). The BDT contains information on the quality of the muon tracks, the relative isolation of the muon, and the vertex the muons are associated with.

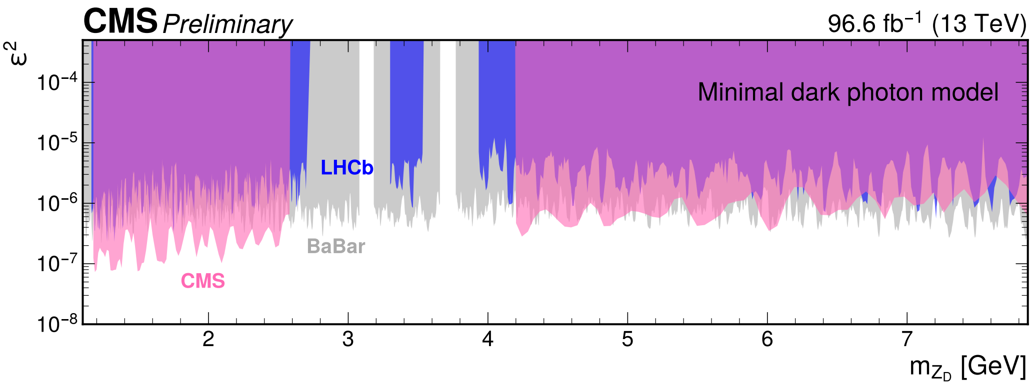

Figure 5: Observed upper limits at 90% CL in the square of the kinetic mixing coefficient ϵ and dark photon mass m_{Z_D} plane in the minimal model of a dark photon (pink). The CMS limits are compared with the existing limits at 90% CL provided by the LHCb experiment [6] (blue) and BaBar experiment [7] (gray).

The signal extraction is performed with a simultaneous signal plus background fits to the di-muon invariant mass distribution, in Fig. 4. The data are found to be consistent with continuum di-muon production. Exclusion limits are provided in the square of the kinetic mixing coefficient and dark photon mass plane, in Fig. 5.

4. Search for inelastic dark matter in events with two displaced muons

The theoretical framework for this analysis is the same as in the previous section. In addition, the dark sector is assumed to be made of two states χ_1 and χ_2 with small mass splitting and with χ_1 being stable. Due to the small mass splitting, χ_2 is long-lived, and decays after travelling a macroscopic distance to a dark photon and χ_1. The analysis targets decay of the dark photon in muon pair because displaced muons are the easiest displaced object to reconstruct due to the location of the muon system at the periphery of the CMS detector. Figure 6 shows the Feynman diagram for the considered production and decay of inelastic dark matter.

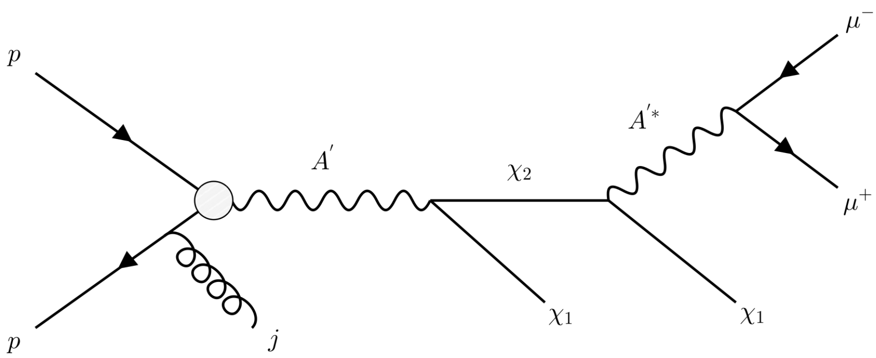

Figure 6: Feynman diagram of inelastic dark matter production and decay for the benchmark signal model considered in proton-proton collisions.

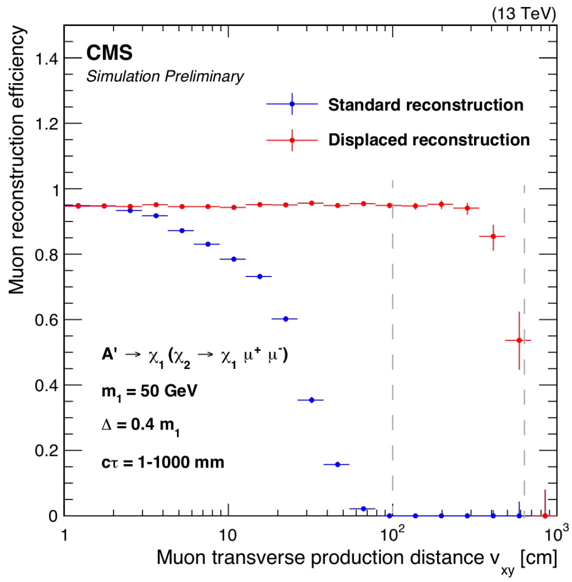

Figure 7: Reconstruction efficiency of standard (blue) and dSA (red) reconstruction algorithms as a function of transverse muon vertex displacement in the central region of the detector ($|\eta| < 1.2$), for a representative signal sample. The two dashed gray lines denote the end of the fiducial tracker and muon chamber regions, respectively.

One of the main features of this analysis is the development of an algorithm designed to reconstruct muons with high efficiency even for large displacements, up to a few meters from the luminous region. This displaced standalone (dSA) algorithm relies solely on muon chamber information. Because the standard global reconstruction algorithm [8] requires both tracker and muon chamber information, it has low reconstruction efficiency for displacement of more than 1 m. Figure 7 shows the reconstruction efficiency of global and dSA muons as a function of the transverse muon vertex displacement.

The event selection targets events with large missing transverse momentum p_T^{miss} aligned with the di-muon system, initial state radiation recoiling off the dark matter system, thus off p_T^{miss}, and two displaced muons with small angular distance. Events are further categorized depending on the number of dSA muons also reconstructed (i.e. matched) as global muons. The backgrounds are estimated using the ABCD method, based on the minimal impact parameter of the two dSA muons and the relative isolation of the matched global muon (2- and 1-match categories) or azimuthal angle between the di-muon system and p_T^{miss} (0-match category). The data is found to be consistent with the expected SM background and exclusion limits in the light state χ_1 mass and interaction strength plane are provided in Fig. 8.

5. Search for resonant production of strongly coupled dark matter

In the case of a dark sector made of strongly coupled dark particles, i.e. dark quarks, a possible experimental signature is semivisible jets [9] (SVJ). SVJ arise in theories where the dark quarks hadronize in the dark sector, forming dark hadrons, a fraction of them decaying promptly to SM

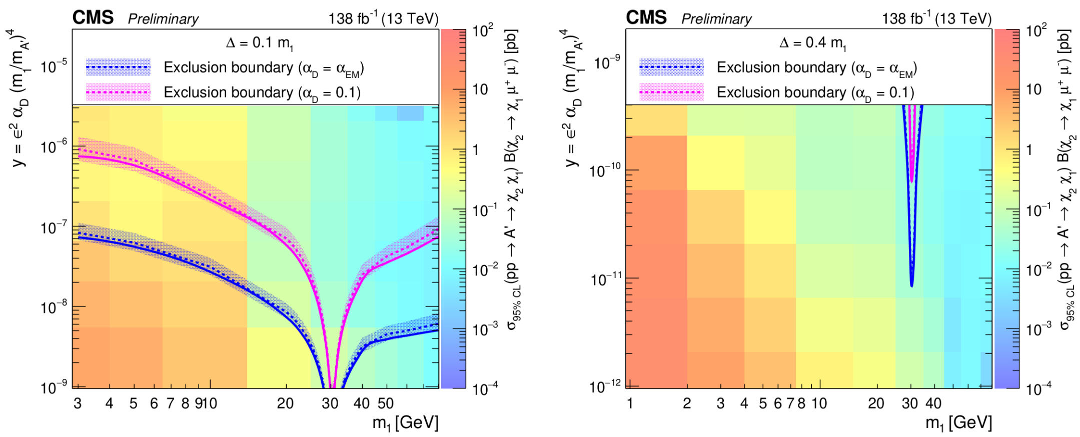

Figure 8: Observed upper limits at 95% CL for $\Delta = m_2 - m_1 = 0.1 m_1$ (left) and $\Delta = 0.4 m_1$ (right) as a function of the light state χ_1 mass m_1 and the interaction strength y. Filled histograms denote observed limits on the product of the dark matter production cross section and decay branching fraction. Regions above the lines are excluded.

quarks which in turns hadronize in the SM sector. The stable dark hadrons escape detection, therefore resulting in missing transverse momentum $p_{\mathrm{T}}^{\mathrm{miss}}$ aligned with a jet in the event. This makes this search orthogonal to "mono-X" searches, targeting events with a visible object recoiling off a DM object. This analysis targets resonant production of SVJs via a vector boson Z' portal, as illustrated in Fig. 9. The main background for the analysis is therefore QCD multijet production, with non-negligible contribution from electroweak processes $t\bar{t}$, W+jets and Z+jets. The search proceeds by tagging SVJ and performing a bump hunt in the transverse mass m_{T} of the di-jet and missing transverse momentum system.

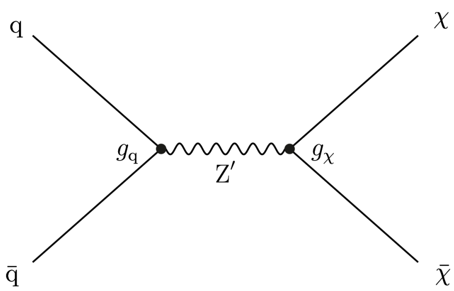

Figure 9: Leading order Feynman diagram of resonant production of dark quark through a Z' mediator.

The event selection targets di-jet events with a small azimuthal angle between the jets and $p_{\mathrm{T}}^{\mathrm{miss}}$, and uses a $R_{\mathrm{T}} = p_{\mathrm{T}}^{\mathrm{miss}}/m_{\mathrm{T}} > 0.15$ selection to reject QCD background. Two signal regions are defined by $0.15 < R_{\mathrm{T}} \leq 0.25$ (low-R_{T}) and $R_{\mathrm{T}} > 0.25$ (high-R_{T}). Furthermore, a SVJ tagger, in the form of a BDT exploiting the differences in jet substructure between SM and semivisible jets, was developed. Signal events are required to have two tagged SVJs, which reduces backgrounds by almost two orders of magnitude.

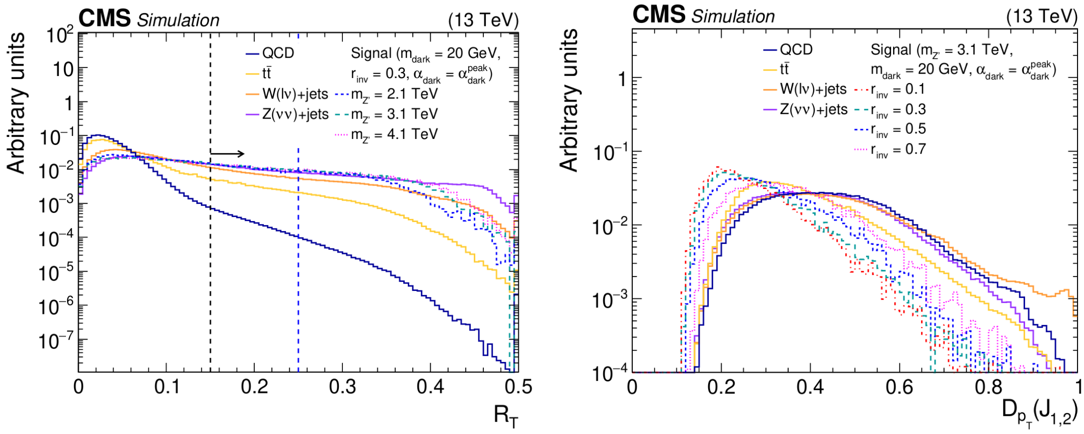

Figure 10: Distribution of R_T (left) and of the transverse momentum dispersion D_{p_T} (right), a jet substructure variable used in the SVJ tagger. The vertical lines in the R_T distribution indicate the two signal regions.

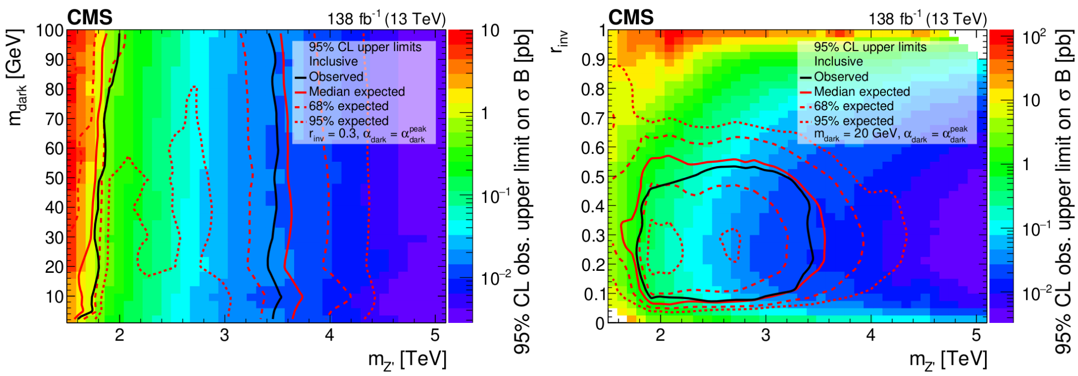

Figure 11: The 95% CL upper limits on the product of the cross section and branching fraction for variations of pairs of the signal model parameters.

The transverse mass m_T distribution is fit to extract the signal strength and estimate backgrounds. No significant deviation from the SM is observed and exclusion limits in terms of the mediator mass $m_{Z'}$, the invisible fraction of dark hadrons r_inv and dark hadron mass m_dark are set in Fig. 11. Model-independent limits, based on the low-R_T and the high-R_T signal regions without application of the SVJ tagger, are also derived.

6. Conclusion

The CMS experiment has an extensive search program for dark matter and hidden sectors. There is no evidence of dark matter at the LHC so far. However CMS continues to explore and exclude uncharted phase-space regions thanks to dedicated data-taking, such as scouting triggers, novel reconstruction and identification algorithms, such as low momentum scouting muons or displaced objects reconstruction, and searches for unexplored experimental signatures, such as semivisible jets.

References

[1] Planck collaboration, *Planck 2018 results. VI. Cosmological parameters*, *Astron. Astrophys.* **641** (2020) A6 [1807.06209].

[2] CMS collaboration, *The CMS Experiment at the CERN LHC*, *JINST* **3** (2008) S08004.

[3] M. Duerr, A. Grohsjean, F. Kahlhoefer, B. Penning, K. Schmidt-Hoberg and C. Schwanenberger, *Hunting the dark Higgs*, *JHEP* **04** (2017) 143 [1701.08780].

[4] CMS collaboration, *Search for a Narrow Resonance Lighter than 200 GeV Decaying to a Pair of Muons in Proton-Proton Collisions at* $\sqrt{s} = 13$ *TeV*, *Phys. Rev. Lett.* **124** (2020) 131802 [1912.04776].

[5] CMS collaboration, *Search for narrow resonances in dijet final states at* $\sqrt{s} = 8$ *TeV with the novel CMS technique of data scouting*, *Phys. Rev. Lett.* **117** (2016) 031802 [1604.08907].

[6] LHCb collaboration, *Search for* $A' \to \mu^+\mu^-$ *Decays*, *Phys. Rev. Lett.* **124** (2020) 041801 [1910.06926].

[7] BaBar collaboration, *Search for a Dark Photon in* e^+e^- *Collisions at BaBar*, *Phys. Rev. Lett.* **113** (2014) 201801 [1406.2980].

[8] CMS collaboration, *Performance of the CMS muon detector and muon reconstruction with proton-proton collisions at* $\sqrt{s} = 13$ *TeV*, *JINST* **13** (2018) P06015 [1804.04528].

[9] T. Cohen, M. Lisanti and H.K. Lou, *Semivisible Jets: Dark Matter Undercover at the LHC*, *Phys. Rev. Lett.* **115** (2015) 171804 [1503.00009].